IEEE Photonics Journal
An IEEE Photonics Society Publication

Misalignment-Tolerant Spot-Size Converter for Efficient Coupling Between Single-Mode Fibers and Integrated Optical Receivers

Volume 4, Number 1, February 2012

Neil Na
Tao Yin

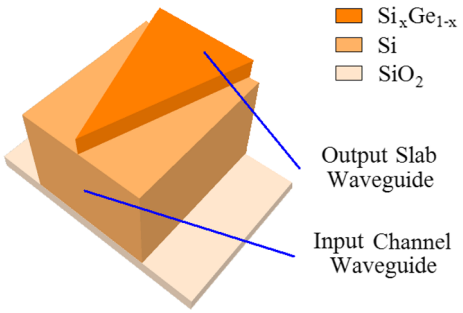

DOI: 10.1109/JPHOT.2012.2183582
1943-0655/$31.00 ©2012 IEEE

Misalignment-Tolerant Spot-Size Converter for Efficient Coupling Between Single-Mode Fibers and Integrated Optical Receivers

Neil Na and Tao Yin

Intel Corporation, Santa Clara, CA 95054 USA

DOI: 10.1109/JPHOT.2012.2183582
1943-0655/$31.00 ©2012 IEEE

Manuscript received November 18, 2011; revised December 31, 2011; accepted January 5, 2012. Date of publication January 9, 2012; date of current version January 25, 2012. Corresponding author: N. Na (e-mail: ycneilna@gmail.com).

Abstract: We design a spot-size converter (SSC) on silicon-on-insulator (SOI) platform to interface an integrated optical receiver (IOR) with a single-mode fiber (SMF). Because of the capability of coupling higher order modes by the proposed device, the tolerance of fiber-to-waveguide misalignment is much improved. The concept is suitable for receivers consisting of multimode-compatible components such as the echelle grating demultiplexer and the Ge waveguide photodetector.

Index Terms: Spot-size converter (SSC), single-mode fiber (SMF), integrated optical receiver (IOR), silicon-on-insulator (SOI), silicon germanium.

1. Introduction

The Si photonics platform has gotten much attention in the research community during the past decade because of its low-cost promise and compatibility with complementary metal-oxide semiconductor electronics. In particular, a large body of work in this field focuses on the problem of how to efficiently couple light into/out of a photonic integrated circuit built upon optical microwaveguides. When a horizontal coupling configuration is considered, it is necessary to construct a spot-size converter (SSC) on chip to interface large external coupling optics, e.g., a single-mode fiber (SMF), to reduce the coupling loss. One approach to solve this problem is to fabricate continuous 3-D Si tapers via grayscale lithography or shadow masking technique [1], [2]. Alternatively, discretized version of these 3-D Si tapers can also be made via multiple Si etch steps [3], [4]. While high coupling efficiencies have been demonstrated using these methods, the topography caused by vertical tapering is undesirable and may cause problems in integrating with other passive/active components. A nanotip or subwavelength structure [5], [6] has also been proposed for efficient coupling, but the required small features may not be compatible with even the most advanced 193-nm optical lithography.

On the other hand, an extra layer of consideration is needed when the SSC is used for an integrated optical receiver (IOR). Because of the uncertainty in the polarization state of incoming light, polarization-dependent loss (PDL) becomes a major issue and has to be minimized. Perhaps, the most straightforward approach is to simply increase the size of optical waveguide to more than a few micrometers, and therefore reduce the difference between TE and TM mode effective refractive indexes. Such a concept has been recently adopted by different groups when making IOR components such as the echelle grating demultiplexer [7], [8] and the Ge waveguide photodetector

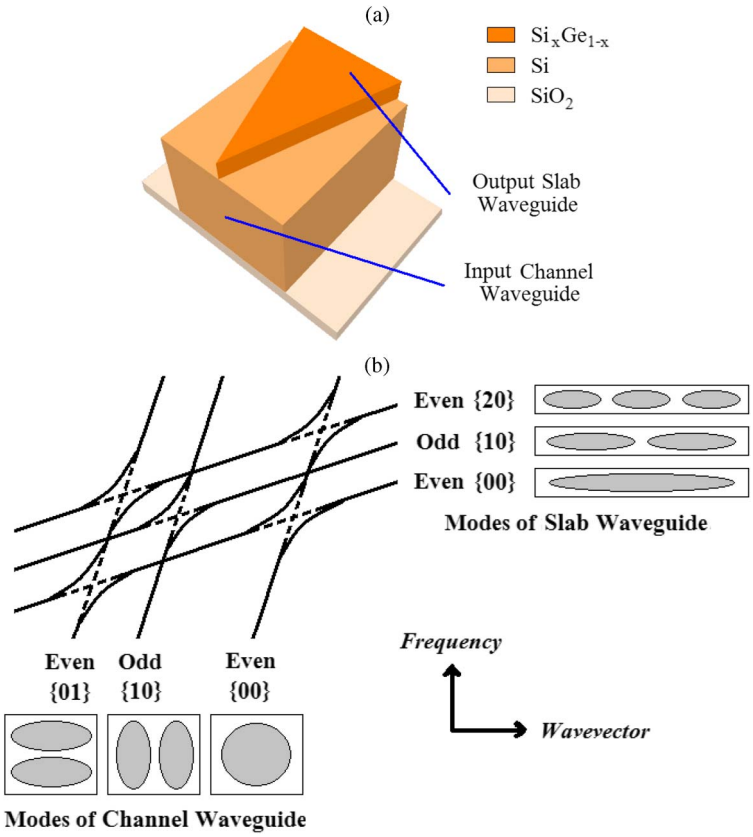

Fig. 1. (a) Schematic plot of the proposed SSC. The actual taper shape is not linear and will be discussed in Section 3. (b) $(k–\omega)$, i.e., wave vector-frequency diagram of the proposed SSC. Mode profiles, mode indexes, and the corresponding parities in the horizontal direction are labeled.

[9], [10]. It is interesting to note that the larger waveguides used in these works are in fact multimode, but the performances are not compromised compared to their single-mode counterparts. In this paper, we take advantage of this concept to design an efficient SSC interfacing an IOR with an SMF. The prominent feature of the proposed SSC is the large tolerance against fiber-to-waveguide misalignment, which is made possible by a multistage inverted-taper design in which the higher-order modes generated by misalignment can be efficiently captured.

2. Device Concept and Misalignment Tolerance

A schematic plot is shown in Fig. 1(a), where the input port is a silicon-on-insulator (SOI) channel waveguide and the output port is a Si_xGe_{1-x} slab waveguide. The Ge composition is assumed to be smaller than 10% so that the absorption loss is negligible at 1310-nm and 1550-nm wavelengths [11]. The core operation principle can be explained in Fig. 1(b), where the dispersion $(k–\omega)$ diagram is plotted for the lowest 3 modes of the channel waveguide (straight lines with larger $d\omega/dk$) and the slab waveguide (straight lines with smaller $d\omega/dk$). Note that for the channel (slab) waveguide, the lowest three modes are {00}, {10}, and {01} ({00}, {10}, and {20}), and their parities along the horizontal direction are labeled accordingly. Because of the evanescent coupling between the channel and the slab waveguides, modes with the same parity in the horizontal direction can interact with each other and cause five normal-mode splittings, as indicated by the dashed lines. From inspecting the resultant waveguide dispersions, one may find that the lowest three modes of the channel and the slab waveguide are connected to each other with one-to-one correspondence. Now, assuming initially the channel waveguide is excited so that the power distributes among the lowest three modes at the bottom of the $(k–\omega)$ diagram. By adiabatically increasing the slab

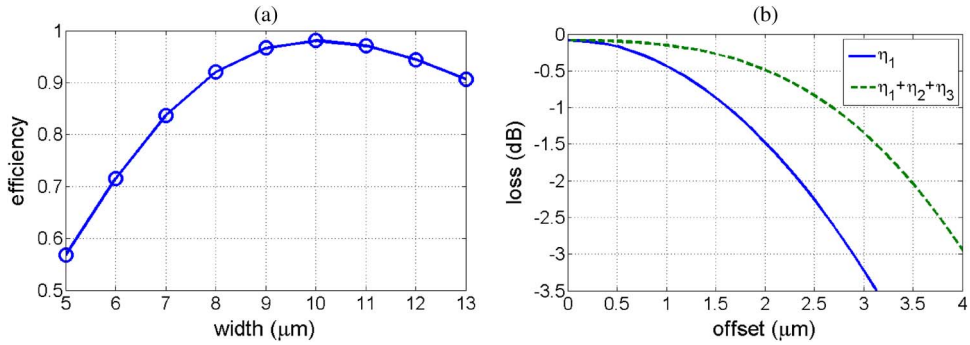

Fig. 2. (a) The fundamental mode coupling efficiency from a standard SMF to a square SOI channel waveguide plotted as a function of square SOI channel waveguide width. (b) The fundamental mode coupling efficiency as a function of fiber-to-waveguide misalignment (blue-solid), and the total power coupling efficiency as a function of fiber-to-waveguide misalignment (green-dashed).

waveguide width, its dispersions can be "pulled" down and eventually sweep across the initial excitation condition and, therefore, coherently transfer the power from the channel waveguide to the slab waveguide. At the moment, we consider only a scalar polarization to illustrate the device concept.

Our device can be regarded as a reminiscence of inverted-taper SSC [12], [13], which is a popular choice in III–V photonics platform due to the ease of adjusting material refractive index. We will show in the following that if the taper transition loss is appropriately managed, our device is capable of increasing the SMF-to-IOR misalignment tolerance by efficiently capturing the higher-order modes. This unique property differentiates our device from those studied in [12] and [13], which are only single-mode compatible. Again, such a design is applicable only if the following IOR components are multimode compatible, as in [7]–[10].

We start with optimizing the width of SOI channel waveguide so that the fundamental mode coupling efficiency from fiber to waveguide can be maximized. This is evaluated by the overlapping integral

$$\eta = \left| \iint F^*(x,y)G(x,y)\,dx\,dy \right|^2 \tag{1}$$

where F and G are the (normalized) fundamental mode profiles of SMF and SOI channel waveguide, respectively. Here, we have made the assumption that an antireflection coating (e.g., HfO_2 for Si–air interface) is applied on the optical facet so that the Fresnel loss is negligible. The core of SMF is 8 μm in diameter with refractive index 1.47 and is surrounded by the cladding with refractive index 1.46. For SOI channel waveguide, the refractive indexes of Si and oxide are assumed to be 3.51 and 1.48, respectively, at 1310-nm wavelength. In Fig. 2(a), we show the fundamental mode overlapping integral as a function of SOI channel waveguide width using (1), where the mode profiles are derived by using eigenmode expansion method [14]. It is found that 98% coupling efficiency can be achieved for 10-μm width, and we will use this number in the following calculations and simulations. Note that a SOI of 10-μm thickness can be implemented by high-temperature epitaxial growth of crystal Si on a commercial submicrometer thick SOI wafer.

The main difference between a conventional inverted-taper SSC [12], [13] and our device is the capability of coupling higher-order modes. Such a feature improves the tolerance of fiber-to-waveguide misalignment: the maximum number of modes may be coupled from a SMF to a square high-index contrast waveguide when there is a fiber-to-waveguide misalignment can be estimated via

$$N_{\max} \sim \frac{1}{4}\pi \cdot NA^2 \Big/ \left(\frac{\lambda}{2w}\right)^2 \tag{2}$$

TABLE 1

Mode conversion efficiencies of four different configurations (from top to bottom): The center of Si_xGe_{1-x} layer is $+0.5$ μm, -0.5 μm, -1.5 μm, or -2.5 μm away from the top surface of SOI channel waveguide. Input modes refer to the modes in SOI channel waveguide; output modes refer to the modes in Si_xGe_{1-x} slab waveguide.

Input \ Output	{00}	{10}	{20}	Total
{00}	4.4%	0	1.9%	6.3%
{10}	0	4.4%	0	4.4%
{01}	12.5%	0	4.6%	17.1%

Input \ Output	{00}	{10}	{20}	Total
{00}	36.4%	0	3.3%	39.7%
{10}	0	34.8%	0	34.8%
{01}	45.9%	0	2.3%	48.2%

Input \ Output	{00}	{10}	{20}	Total
{00}	50.0%	0	2.3%	52.3%
{10}	0	61.3%	0	61.3%
{01}	40.1%	0	16.2%	56.3%

Input \ Output	{00}	{10}	{20}	Total
{00}	66.9%	0	1.9%	68.8%
{10}	0	77.3%	0	77.3%
{01}	28.3%	0	21.8%	50.1%

where *NA* is the numerical aperture of a SMF, λ is the free-space wavelength, and w is the width of a square high-index contrast waveguide. The division in (2) counts the number of modes in k space bounded by the *NA* of a SMF. The 1/4 prefactor is one quarter of a circle with radius equal to *NA*. The polarization degeneracy is neglected. Consider a standard SMF with $NA = 0.14$ and assuming $\lambda = 1310$ nm and $w = 10$ μm, N_{max} is ~ 3.58; therefore, only the lowest three modes can be coupled when there is a fiber-to-waveguide misalignment. In Fig. 2(b), we show the overall coupling efficiency (from fiber to channel waveguide to slab waveguide) of the fundamental mode or the lowest three modes as a function of fiber-to-waveguide misalignment, assuming the SSC efficiency (from channel waveguide to slab waveguide) is unity. A conventional inverted-taper SSC corresponds to the case where only the fundamental mode is considered, and our device corresponds to the case where the lowest three modes are considered. It is found that the fiber-to-waveguide misalignment tolerance is much improved in case of our device, e.g., at 3-μm offset, there is about 2-dB improvement over the conventional inverted-taper SSC. Such a feature can greatly reduce the optical coupling loss when practical packaging misalignments are taken into consideration. In the next section, we'll show how to implement such a coupling concept via multistage inverted-taper design where high SSC efficiency can be obtained.

3. Device Design and Simulation

To evaluate the performance of the proposed SSC, we perform mode propagation simulations based on scattering matrix technique [14]. We consider four different configurations where the Si_xGe_{1-x} layer centers are located at $+0.5$ μm, -0.5 μm, -1.5 μm, and -2.5 μm from the top Si surface. Note that the heights are all 1 μm thick so the Si_xGe_{1-x} layer is buried in Si matrix for the latter two cases. As a first example, the Si_xGe_{1-x} layer widths are all linearly tapered from 200 nm to 7 μm. The refractive indexes are 3.54, 3.54, 3.52, and 3.52, respectively, which are chosen so that the lowest three modes in Si will all be trapped by Si_xGe_{1-x} at a common propagation distance about 1 mm. TM polarization is used. We summarize the simulation results in Table 1, and find in general, the deeper the Si_xGe_{1-x} layer the larger the mode conversion efficiency. This is expected because by pushing the Si_xGe_{1-x} slab waveguide into the SOI channel waveguide, the mode

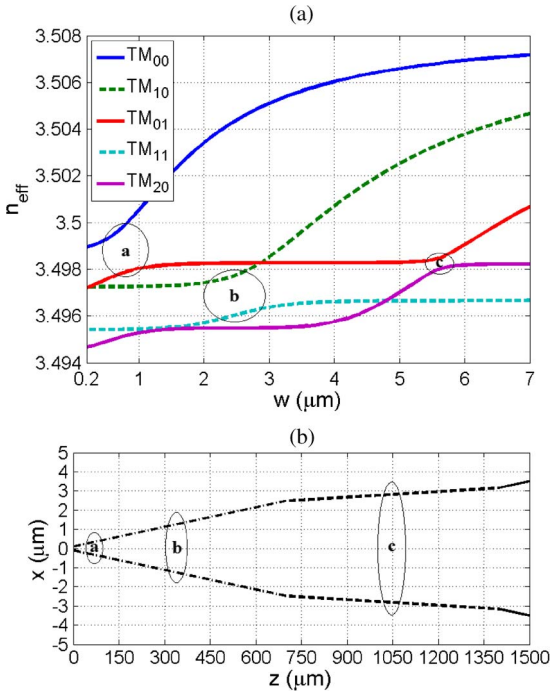

Fig. 3. (a) The waveguide effective index plotted as a function of Si_xGe_{1-x} layer width with different input modes. (b) The designed multistage taper for efficient coupling from SOI channel waveguide to Si_xGe_{1-x} slab waveguide. The circled **a**, **b**, and **c** regions correspond to the locations of normal-mode splittings.

overlapping between them is improved so that the normal-mode splittings shown in Fig. 1(b) becomes larger. The mode-to-mode scattering coefficient due to nonadiabaticity [15]

$$C_{ij}(z) = \frac{1}{4}\frac{1}{n_{eff}^{i}(z) - n_{eff}^{j}(z)} \times \int \frac{\overset{v}{E}_i^{*}(x,y) \cdot \overset{v}{E}_j(x,y)}{Z_o}\frac{\partial n(x,y,z)^2}{\partial z}\, dx\, dy \tag{3}$$

is therefore reduced due to a larger effective index difference (the term in (3) before the integral) at the normal-mode splittings. Note that nevertheless, nonadiabaticity is not always detrimental to the total coupling efficiency. As an example, when TM_{01} is the input mode it should be completely converted to the output mode TM_{20} under an adiabatic transition. If the system is not fully adiabatic, some power of the input mode TM_{01} can be scattered to the output mode TM_{00}, which is still being trapped by the Si_xGe_{1-x} layer and therefore contributes to the total coupling efficiency. Such a delicate feature makes the design of the proposed SSC more complicated compared to a conventional inverted-taper SSC, and a deeper understanding of the intermode power transfer is essential.

To further understand the mechanism of intermode power transfer in the proposed SSC, we calculate the individual mode powers along the propagation path for input modes TM_{00}, TM_{10}, and TM_{01}. The structure where the Si_xGe_{1-x} layer is -2.5 μm below the top Si surface is assumed. It is found that at $z \sim 100$ μm, 350 μm, and 800 μm, e.g., $w \sim 0.7$ μm, 2.45 μm, and 5.6 μm for linear tapering, the intermode power transfer is rather severe. These locations correspond to the normal-mode splittings in Fig. 1(b), and can be clearly identified by plotting the eigenmode effective index as a function of Si_xGe_{1-x} layer width, as shown in Fig. 3(a).

Based on the above information, we design a SSC featuring uniform coupling losses for the lowers three modes. The Si_xGe_{1-x} layer is -2.5 μm below the top Si surface.[1] Its width is first

[1]This buried structure will require Si_xGe_{1-x} epitaxy growth and etching, followed by Si epitaxy growth and chemical-mechanical polishing.

TABLE 2

Mode conversion efficiencies of the designed single-stage (top) and multistage (bottom) inverted-tapers

Input \ Output	{00}	{10}	{20}	Total
{00}	67.0%	0	1.8%	68.8%
{10}	0	77.3%	0	77.3%
{01}	28.3%	0	21.8%	50.1%

Input \ Output	{00}	{10}	{20}	Total
{00}	65.9%	0	11.3%	77.2%
{10}	0	77.3%	0	77.3%
{01}	30.5%	0	48.0%	78.5%

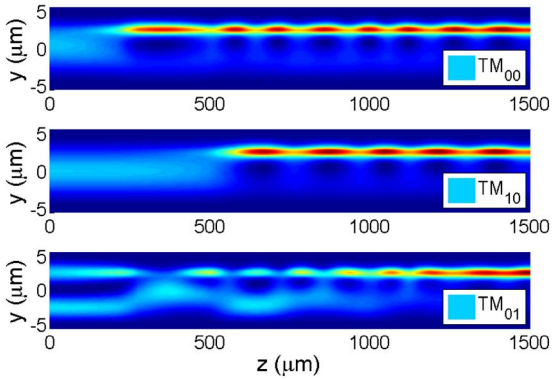

Fig. 4. Intensity profiles on the yz-plane for input modes TM_{00}, TM_{10}, and TM_{01} (from top to bottom) using multistage inverted-taper.

tapered from 200 nm to 4.96 μm in a length of 700 μm, then tapered from 4.96 μm to 6.32 μm in a length of 700 μm, and finally tapered from 6.32 μm to 7 μm in a length of 100 μm. All three tapers are linear in shape, and the structure is shown in Fig. 3(b). While the taper slopes for the first and the third ones remain the same as in the previous design, the taper slope for the second one is now 3.5 times smoother. This way, we minimize the mode-to-mode scattering at $w \sim 5.6$ μm in which only a small normal-mode splitting exists (see c in Fig. 3). The simulation results are summarized in Table 2, and uniform coupling losses for the lowest 3 modes as small as $\sim$1.1 dB are obtained for this new design. Further reduction of the coupling losses can be done by proportionally increasing the taper lengths. In Fig. 4, we plot the intensity profiles in the yz-plane to visualize the mode conversions. It starts with a large SOI channel waveguide mode at the input facet and then converts to a small Si_xGe_{1-x} slab waveguide mode during propagation. Again, the propagation distance (or Si_xGe_{1-x} layer width) in which the spot-size shrinks significantly corresponds to the location of normal-mode splitting, which can be identified by a comparison between Figs. 3 and 4. We have also performed similar simulations using input modes TE_{00}, TE_{10}, and TE_{01}, and found less than 5% of PDL for all them. Furthermore, the spectral 1-dB full-widths for the lowest three modes are determined to be at least larger than 150 nm, and therefore, the proposed SSC is suitable for a variety of wavelength-division multiplexing applications.

4. Conclusion

An SSC capable of efficiently coupling higher-order modes on Si photonics platform is proposed and analyzed, which is made possible by a multistage inverted-taper design. Total coupling loss as low as 1.1 dB can be achieved for the lowest three modes, along with a large 5.5-μm 1-dB full-width misalignment tolerance. The large tolerance of fiber-to-waveguide misalignment makes our device

a unique optical interface between a SMF and an IOR. Note that the device concept can be applied to other material system such as III–V photonics platform as well. Finally, we emphasize that the IOR itself has to be multimode compatible to fully benefit from our device. This is true for recently demonstrated IOR components such as the echelle grating demultiplexers and the Ge waveguide photodetectors using high-index contrast waveguides with width about a few micrometers.

References

[1] A. Sure, T. Dillon, J. Murakowski, C. Lin, D. Pustai, and D. W. Prather, "Fabrication and characterization of three-dimensional silicon tapers," *Opt. Exp.*, vol. 11, no. 26, pp. 3555–3561, Dec. 2003.

[2] A. Harke, T. Lipka, J. Amthor, O. Horn, M. Krause, and J. Müller, "Amorphous silicon 3-D tapers for Si photonic wires fabricated with shadow masks," *IEEE Photon. Technol. Lett.*, vol. 20, no. 17, pp. 1453–1454, Sep. 2008.

[3] D. Dai, S. He, and H.-K. Tsang, "Bilevel mode converter between a silicon nanowire waveguide and a larger waveguide," *J. Lightw. Technol.*, vol. 24, no. 6, pp. 2428–2433, Jun. 2006.

[4] A. Barkai, A. Liu, D. Kim, R. Cohen, N. Elek, H.-H. Chang, B. H. Malik, R. Gabay, R. Jones, M. Paniccia, and N. Izhaky, "Double-stage taper for coupling between SOI waveguides and single-mode fiber," *J. Lightw. Technol.*, vol. 26, no. 24, pp. 3860–3865, Dec. 2008.

[5] V. R. Almeida, R. R. Panepucci, and M. Lipson, "Nanotaper for compact mode conversion," *Opt. Lett.*, vol. 28, no. 15, pp. 1302–1304, Aug. 2003.

[6] P. Cheben, D.-X. Xu, S. Janz, and A. Densmore, "Subwavelength waveguide grating for mode conversion and light coupling in integrated optics," *Opt. Exp.*, vol. 14, no. 11, pp. 4695–4702, May 2006.

[7] W. Wang, Y. Tang, Y. Wang, H. Qu, Y. Wu, T. Li, J. Yang, Y. Wang, and M. Liu, "Etched-diffraction-grating-based planar waveguide demultiplexer on silicon-on-insulator," *Opt. Quantum Electron.*, vol. 36, no. 6, pp. 559–566, May 2004.

[8] D. Feng, W. Qian, H. Liang, C.-C. Kung, J. Fong, B. J. Luff, and M. Asghari, "Fabrication insensitive echelle grating in SOI platform," *IEEE Photon. Technol. Lett.*, vol. 23, no. 5, pp. 284–286, Mar. 2011.

[9] T. Yin, R. Cohen, M. Morse, G. Sarid, Y. Chetrit, D. Rubin, and M. J. Paniccia, "31 GHz Ge n-i-p waveguide photodetectors on silicon-on-insulator substrate," *Opt. Exp.*, vol. 15, no. 21, pp. 13 965–13 971, Oct. 2007.

[10] D. Feng, S. Liao, P. Dong, N.-N. Feng, H. Liang, D. Zheng, C.-C. Kung, J. Fong, R. Shafiiha, J. Cunningham, A. V. Krishnamoorthy, and M. Asghari, "High-speed Ge photodetector monolithically integrated with large cross-section silicon-on-insulator waveguide," *Appl. Phys. Lett.*, vol. 95, no. 26, p. 261 105, Dec. 2009.

[11] R. Braunstein, A. R. Moore, and F. Herman, "Intrinsic optical absorption in germanium-silicon alloys," *Phys. Rev.*, vol. 109, no. 3, pp. 695–710, Feb. 1958.

[12] R. N. Thurston, E. Kapon, and A. Shahar, "Two-dimensional control of mode size in optical channel waveguides by lateral channel tapering," *Opt. Lett.*, vol. 16, no. 5, pp. 306–308, Mar. 1991.

[13] I. Moerman, P. P. Van Daele, and P. M. Demeester, "A review on fabrication technologies for the monolithic integration of tapers with III-V semiconductor devices," *IEEE J. Sel. Topics Quantum Electron.*, vol. 3, no. 6, pp. 1308–1320, Dec. 1998.

[14] D. F. G. Gallagher and T. P. Felici, "Eigenmode expansion methods for simulation of optical propagation in photonics—Pros and cons," in *Proc. SPIE*, Jan. 2003, vol. 4987, pp. 69–82.

[15] A. W. Snyder and J. D. Love, *Optical Waveguide Theory*. London, U.K.: Chapman & Hall, 1983.